

# DEVELOPMENT OF SOFTWARE TOOLS FOR CONSEQUENCE ASSESSMENT OF AERIAL RADIOACTIVE DISCHARGES

Petr Pecha<sup>1</sup>, Radek Hofman<sup>1</sup>, Petr Kuča<sup>2</sup>, Kateřina Zemánková<sup>3</sup>

<sup>1</sup> *Institute of Information Theory and Automation, AV ČR, Prague*

<sup>2</sup> *National Radiation Protection Institute, Prague*

<sup>3</sup> *Faculty of Mathematics and Physics, Charles University, Prague*

## Introduction

This article describes the latest research achievements in the field of modelling of radioactivity propagation through the living environment. Systematic development of the code HAVAR aimed to improved description of uncertainty propagation through the mathematical model has resulted into probabilistic version HAVAR-RP (Reliability Predictions) [5]. It has markedly facilitated an implementation of advanced tendencies into the modelling, mainly, the transition from deterministic consequence assessment to probabilistic approach. Detailed analysis of the model error covariance structure has prepared right basis for application of the modern statistical methods for assimilation of real measurements on terrain with the model predictions. The successor of the environmental model HAVAR-RP is designated as HARP (Hazardous Radioactivity Propagation). The product offers extensive interactive software tools for input definitions of the model parameters (for release scenario definitions, dispersion and deposition submodels, dynamic ingestion). The user friendly output subsystem provides an interactive tool for browsing of nearly all conceivable results important for decision makers (conversational mode on basis on “user demands”).

The HARP system represents the application part of the grant project supported by Grant Agency of the Czech Republic (period 2007–2009), which was solved in the Institute of Information Theory and Automation, AV ČR. The advanced statistical methods developed within the grant project for assimilation of measurements with model predictions in the early and late phases of a radiation accident are incorporated into the assimilation subsystem. The HARP system is tuned and tested in cooperation with National Radiation Protection Institute in Prague, where the product is online connected to the ORACLE database server and can input directly meteorological data (including short term 3-dimensional meteorological forecast). For the purposes of testing of assimilation procedures, the measurements in terrain are simulated “artificially”.

## Practice in modelling of atmospheric dispersion of pollution and its deposition on terrain

Models of pollution transport in atmosphere towards human body constitute a significant prerequisite tool for decision support. Various models of radioactivity propagation originally discharged into the atmosphere are able to incorporate fundamental features of the problem under different approaches. It relates to dimensionality, calculation domain and grid resolution, parametrization of respective physical phenomena, initial and boundary conditions, intensive computation techniques. It is evident, that a certain compromise between complexity and exactness of methodology, computer code speed and attained accuracy of the results has to be recognised. Inherent constraints of the models capability arise from

embedded uncertainties, limited information about the source of contamination, stochastic character of atmospheric phenomena, limited time for generation of a reliable prediction etc. An illustration of complexity of the waste plume tracking over the terrain and its concentration depletion due to dispersion and admixture decay, washout and dryout (dry deposition) is given in Figure 1.

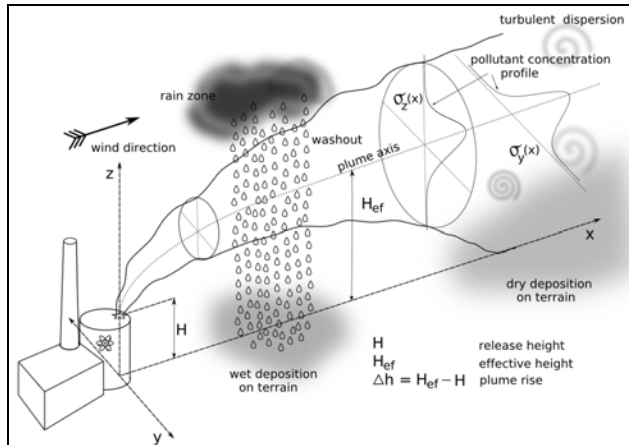


Figure 1: Illustration of complex phenomena during propagation of harmful substances initially discharged into the atmosphere

Various approaches to solution of the pollution transport are developed in dependency on the purpose of analysis. It covers various domains with different scales and typical resolutions from microscale ( $\sim 200 \times 200 \times 100$  m ; grid resolution 5 m or less) through mesoscale ( $\sim 100 \times 100 \times 5$  km ; 2 km ) up to regional ( $\sim 1000 \times 1000 \times 10$  km ; 20 km) or continental or global. The atmospheric dispersion models can be distinguished according to their characteristics related to (i) coordinate systems (Eulerian or Lagrangian), (ii) resolution of wind field, and (iii) averaging (respecting spatial and temporal scales of fluid-mechanical phenomena). From the historical point of view, in relation with computer development in the 1970s, the Gaussian plume solutions were investigated. In the 1980s, the development of Lagrangian puff models has started, as well as improvement of three dimensional Eulerian schemes (with few grid nodes). The 1990s achieved great advance in 3-D Eulerian models linked with numerical weather prediction models.

### The purpose of application determinates the choice of model

At present, several general models types are used: plume, segmented plume, puff, Lagrangian particle, Eulerian grid and some other special. The classical **Gaussian approach** is still alive and successfully applied in many branches. The models have long tradition of their use for dispersion predictions of continuous, buoyant air plume originating from ground-level or elevated continuous sources of pollution. Gaussian models can be used for non-continuous sources and changing meteorology in modification of so called puff approach or segmented plume scheme. Even simple, the Gaussian model is consistent with the random nature of turbulence, it is a solution of Fickian diffusion equation for constant  $K$  and  $u$ , the model is tuned to experimental data and offers fast basic estimation with minimum computation effort. Proved semi-empirical formulas are available for approximation of important effects like interaction of the plume with *near-standing buildings*, momentum and buoyant *plume rise* during release, power-law formula for estimation of wind speed *changes with height*, *depletion* of the plume activity due to *removal processes* of dry and wet depositions and radioactive decay, dependency on *physical-chemical forms* of admixtures and *land-use*

*characteristics*, simplified account of *inversion* meteorological situation and plume *penetration of inversion*, plume *lofting* above inversion layer, account for small changes in *surface elevation*, *terrain roughness* etc.

**Lagrangian** dispersion models are naturally suited to dispersion problems. Their reference system follows the prevailing vector of atmospheric flow. The *Lagrangian particle dispersion* model tracks each “point-like” particle of pollution on its path through atmosphere. The particles are drifted with the mean wind velocity and are additionally subjected to the random turbulence. The concentration distribution is determined by counting the particles in a given sampling volumes. Advanced effective modification for mesoscale modelling is *Puff Particle Model* (PPM) using concept of relative diffusion of a puff. Pollution source quantities are joined together by a puff (a parcel of particles) containing finite number of infinitesimal particles. Each particle moves due to the mean fluid velocity of the puff and due to the turbulent sub-grid scale velocity. Lagrangian trajectories are numerically simulated for great number of these particles and the particles in given sampling volumes are finally counted. As large number of particles has to be simulated ( $10^4 - 10^5$ ), the methods require powerful computational tool.

**Eulerian** dispersion models solve the pollutant problem described by diffusion equation in a framework of fixed 3-D Cartesian equidistant computation grid. The concentration of pollution is simulated in an array of fixed Earth-based computational cells. The method can give detailed information on concentration distribution even if complex boundary conditions in the microscale domain are involved. Eulerian approach is greatly computationally expensive and sometimes numerical problems can arise.

Lagrangian or Eulerian model represents suitable tool for detailed modelling at short distances and complex boundary conditions. Especially, the specific present-day development is oriented on analysis of hypothetical terrorist attacks with RDD in urban areas. The models can be nested within the Gaussian model which can describe the further propagation in longer distances from the source. The primary dispersion algorithm developed specially for the HARP system is based on a segmented Gaussian scheme [7,8]. The main objective consists in development of as fast as possible and accurate enough computer code for purposes of not only deterministic estimation, but mainly for multifold repetitive sequential Monte Carlo calculations (for many thousand realisations of random model parameters). Such code constitutes inevitable prerequisite for probabilistic assessment and application of advanced statistical assimilation techniques of Bayesian filtering.

### **Proper and up-to-date data for advanced modelling**

A basic prerequisite for utilization of the advanced models is availability of the latest formats of all inputs such geographical and demographical databases, measurements from terrain, estimation of the source term, vegetation periods and many others. But cardinal role for the correct assessment of accident consequences plays incorporation of a proper description of the atmospheric flow fields. The mathematical model should conform to all details of the current meteorological forecasts. More informative meteorological data also enables to improve the former classical Gaussian approach (direct evaluation of atmospheric turbulence through the friction velocity and Monin-Obukhov length).

Earlier in 1904, V. Bjerkens pointed out that there is a complete set of seven equations with seven unknowns that governs the evolution of state in atmosphere represented by 3 momentum conservation equations for each wind velocity component, continuity equation, the equation of state of ideal gases, energy conservation and water vapour mass conservation. At the same time this differential equation system describes a chaotic nature that impose limit on stability of weather predictions and weather predictability at all. In a chaotic system, the introduced errors can grow with time. This represents ultimate problem in meteorological

forecasting. Just assimilation of the meteorological measurements with weather predictions has been found as an efficient technique in the struggle against tendency to destruction of model knowledge.

The environmental model HARP is online connected to meteorological data provided by the Czech Hydro-Meteorological Institute. For JE Dukovany and JE Temelín both point and gridded (160 × 160 km, ALADIN format) short term forecast (48 hours forward) are at the disposal. Several comparisons of SGPM results with HYSPLIT code [2] (HYbrid Single-Particle Lagrangian Integrated Trajectory model) have been accomplished within the grant project. A proper sequence of the 3-D meteorological forecast in MM5 format entering the HYSPLIT calculations was obtained thanks to cooperation with specialists from the MEDARD project from the Institute of Computer Science, AV ČR. The illustrative partial results are shown in Figure 2. Having simultaneous real measurements for this period, sometimes distinct difference has occurred among wind field predicted by ALADIN, predicted by MM5 and the real onsite measurements. Probably, the gridded meteorological data (provided on grid mesh 9 × 9 km) sometimes are not capable to catch properly the local changes. The need for some kind of intelligent meteorological pre-processor is evident.

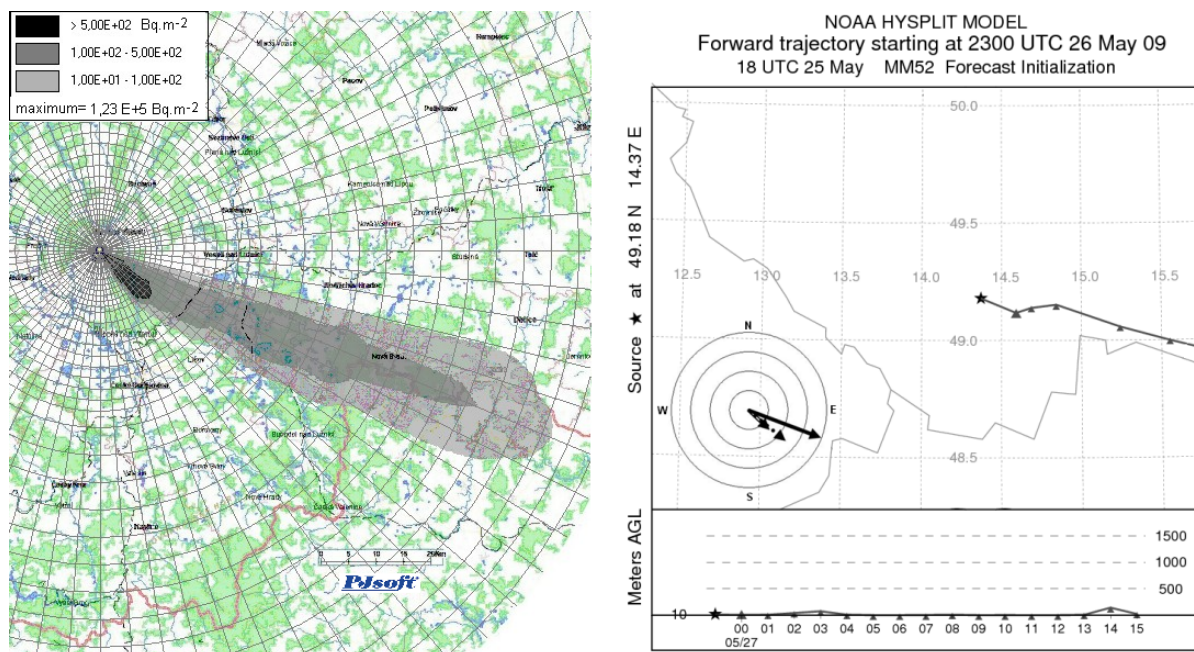


Figure 2: Hypothetical release of  $^{131}\text{I}$  for real meteorology from May 26, 2009, release start at 23.00 UTC. Duration of release is 1 hour, discharged activity  $6.0\text{E}+11$  Bq. Left: Segmented Gaussian plume model with limited 3-D ALADIN short term forecast (trace of  $^{131}\text{I}$  deposition on terrain after 5 hours). Right: Trajectory of the cloud for the same situation and scenario calculated by HYSPLIT code [2] with 3-D meteorological forecast in MM5 format. Wind rose in left-bottom corner stands for wind direction for the first hour: forecast from ALADIN (double line), forecast from MM5 (solid line), real measurements (dotted line).

### Segmented Gaussian Plume model (SGPM) of aerial transport

Air born admixtures are drifted by the surrounding ambiance and, precisely, the equation describing the pollution transport should be solved simultaneously together with the equations describing the state of atmosphere. Because of the practical infeasibility, the pollution transport is analyzed separately whereas the meteorological fields enter the calculations externally as input. Analytical solution of diffusion equation can be found only under the drastic simplifications and for simple initial and boundary conditions.

Our approach is based on Gaussian dispersion modelling using further modifications of a certain numerical scheme which ensures an accounting for the real situation. A basic idea insists in synchronization of available short-term meteorological forecast provided by the Czech meteorological service with release dynamic of harmful substances discharged into the atmosphere. Real dynamics of accidental release is transformed into an equivalent number  $G$  of consecutive homogeneous segments with duration 1 hour. Movement of each segment is driven by short-term meteorological forecast for corresponding hours of propagation. The shape of the segment spreading is simulated by “Gaussian droplet” coming out from the simplified solution of the diffusion equation.

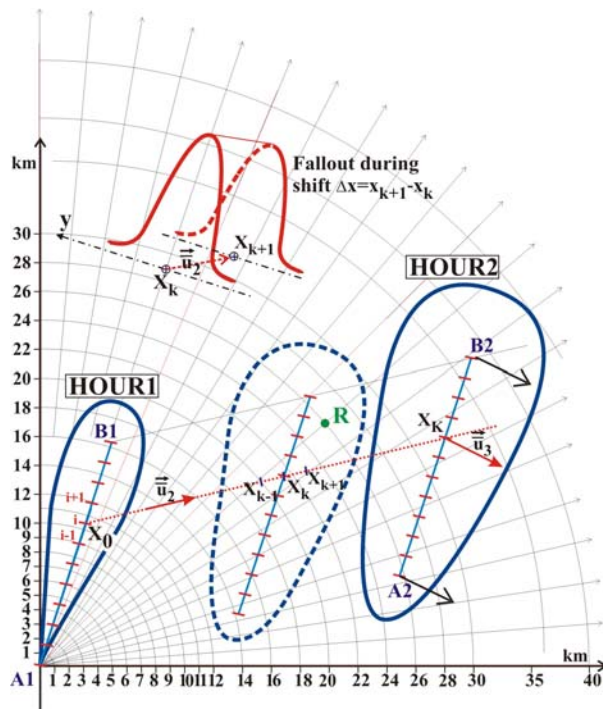


Figure 3: Segmented Gaussian plume approach for modelling of discharges propagation in atmosphere

The principle of the numerical algorithm SGPM originally developed for the HARP system is illustrated in Figure 3. Total movement of each partial Gaussian one-hour segment within the next subsequent one-hour interval is modelled as a sequence of partial elemental shifts  $k$  ( $k=1, \dots, K$ ;  $K = 30 \div 50$ ). Let follow the one-hour segment in its position just after the 1<sup>st</sup> hour of motion. The position is in Figure 3 designated as HOUR1. We describe it according to the Gaussian straight-line approximation in 1-hour prolongation (“Gaussian droplet”). Meteorological forecast for the second hour is used and the HOUR1-segment is drifted during the whole second hour according to the wind vector  $u_2$ , class of atmospheric stability  $class_2$  and precipitation intensity  $v_2$ . The “droplet” movement from position HOUR1 to HOUR2 is then modelled as a sequence of  $K$  partial shifts starting from known initial position on the plume segment HOUR1 with axis (A1;B1) up to HOUR2 with axis (A2;B2). Near-ground activity concentration in air  $C$  ( $Bq \cdot m^{-3}$ ) of a certain radionuclide is calculated step by step after each elemental shift  $k$ .

SGPM uses “source depletion” approach based on separation of the pure dispersion solution  $C^{disper}$  and “removal” component given by the plume depletion factors  $f_R^n, f_F^n, f_W^n$  due to the radioactive decay ( $R$ ) and dry ( $F$ ) and wet ( $W$ ) deposition in dependence on physical-chemical form of the nuclide  $n$  (index  $n$  further omitted in this paragraph). Decrease of activity

concentration within the elemental shift  $k \rightarrow k + 1$  of the droplet can be described schematically by separation of pure dispersion component  $C^{disper}$  and the depletion factors:

$$\begin{aligned}
 C(X_{k+1}) &= C^{disper}(X_{k+1}) \cdot \Delta f_R^{k \rightarrow k+1} \cdot \Delta f_F^{k \rightarrow k+1} \cdot \Delta f_W^{k \rightarrow k+1} \\
 \left. \begin{aligned}
 \text{Rad. decay: } \Delta f_R^{k \rightarrow k+1} &= \exp(-\lambda |X_{k+1} - X_k| / u_2) \\
 \text{Dryout: } \Delta f_F^{k \rightarrow k+1} &= 1 - \sqrt{2/\pi} \frac{v_g \left( \overline{X^{k,k+1}} \right)}{u_2 \sigma_z \left( \overline{X^{k,k+1}} \right)} \exp \left[ \frac{H_{ef}^2}{2\sigma_z^2 \left( \overline{X^{k,k+1}} \right)} \right] \\
 \text{Washout: } \Delta f_W^{k \rightarrow k+1} &= \exp(-\Lambda |X_{k+1} - X_k| / u_2)
 \end{aligned} \right\} \quad (1)
 \end{aligned}$$

Gaussian solution for  $C^{disper}(X_{k+1})$  is derived in [7,8],  $\lambda$  stands for decay constant, washout coefficient is marked as  $\Lambda$ , effective height of the plume is  $H_{ef}$ . Dry deposition velocity  $v_g$  and vertical dispersion coefficient  $\sigma_z$  are related to the centre of abscissa  $\overline{X^{k,k+1}}$ , distance of the points  $X_k, X_{k+1}$  is denoted as  $|X_k - X_{k+1}|$ .

Determination of contribution of the segment to the TIC (Time Integral of near ground activity Concentration) value in receptor point R during its movement from partial position  $k$  to the next partial position  $k+1$  is expressed as:

$$\Delta TIC(R; k) = \frac{C(R, k) + C(R, k+1)}{2} \cdot \Delta t(k) \quad (2)$$

Time difference  $\Delta t(k) = |X_k - X_{k+1}| / \bar{u}_2$  is set equal for each  $k$ . TIC value at receptor point R from all consecutive partial shifts  $k, k=1, \dots, K$  is given by:

$$TIC(R; K) = \sum_{k=1}^K \Delta TIC(R; k) \quad (3)$$

Similar considerations concerning activity deposition on terrain around receptor point R can be adopted. Deposited activity at receptor point R due to dry and wet effects during elemental shift  $\Delta t(k)$  is approximated as:

$$\Delta DEP(R; k) = \Delta DEP^{dry} + \Delta DEP^{wet} \quad (4)$$

Contribution from dry fallout:

$$\Delta DEP^{dry} = \Delta TIC(R; k) \cdot v_g \quad (4a)$$

Contribution from the wet deposition in BOX model approach (full vertical homogenization along mixing layer with height  $H_{mix}$ ):

$$\Delta DEP^{wet} = \Delta TIC(R; k) \cdot \Lambda \cdot H_{mix} \quad (4b)$$

Deposited activity at receptor R just in the time of shift  $k$  is sum of deposited activity from all previous shifts  $j$  starting from position HOUR1 for  $j=1$  up to monitoring shift  $k$ . Taking into account radioactive decay, activity deposition just in time of the shift  $k$  is given by:

$$DEP(R; k) = \sum_{j=1}^k \{ \Delta DEP(R; j) \cdot \exp[-\lambda(k-j) \cdot \Delta t] \} \quad (5)$$

Deposited activity at receptor R after the whole movement of segment from its position HOUR1 to HOUR2 is denoted as  $DEP(R, K)$  is calculated according to the previous equation

after substitution  $k=K$ . Now we can determine the time integral of deposited activity during the whole movement of the plume segment from HOUR1 to HOUR2 as:

$$\text{TID}(R;K) = \sum_{k=1}^K \{ \text{DEP}(R;k) \cdot \Delta t \} \quad (6)$$

The basic SGPM model of aerial transport of radioactivity has been verified by extensive comparative analysis [5] including COSYMA and RODOS runs.

An example of SGPM calculation is given in Figure 4 for the following fictive imaginary scenario: release of radionuclide  $^{131}\text{I}$  from NPP Dukovany; release start on June 25, 2008, 17.00 CET (summer storm with rather fast meteorological changes). The release duration is assumed 1 hour, total activity release of  $^{131}\text{I}$  into atmosphere is  $7.48\text{E}+13$  [Bq], release height is 45 m, dispersion is calculated for smooth terrain of European type (SCK/CEN formulae). Two kinds of short-term meteorological forecasts are generated and transmitted from CHMI to the ORACLE database:

**Scheme 2:** Simple short-term meteorological forecast for single reference point of NPP. Each hourly segment of release is driven by hourly meteorological conditions that are changing in time (each hour) but applied in the same way in the whole region at once (*time dependant, spatially constant*).

**Scheme 3:** Gridded 2-D and 3-D meteorological data on mesoscale region  $160 \times 160$  km around each NPP. Each hourly segment of release is driven by hourly meteorological conditions that are changing in time (each hour) and space (*time dependant, spatially dependant*).

SGPM algorithm is capable to accept both schemes. The scheme in Fig. 4 subjects the “Gaussian droplet” to translation, rotation and squeezing during its transport in the successive 1-hour meteorological phases. We can expect better determination of affected areas when more precise (scheme 3 gridded data) meteorological forecast is used [8].

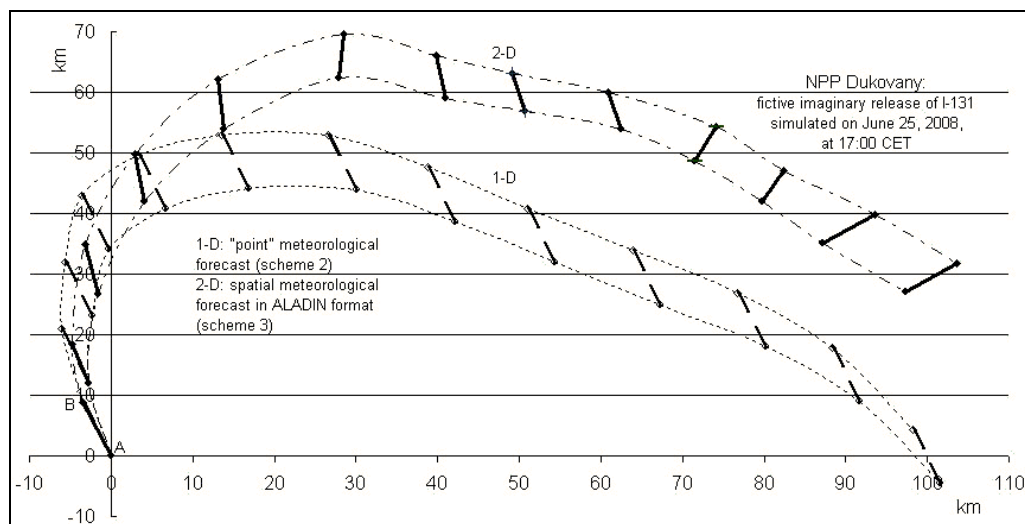


Figure 4. Abscissa AB illustrates trace of  $^{131}\text{I}$  plume in the first hour of release. Its stepwise movement in the next hours is modelled alternatively using 1-D meteorological forecast (Scheme 2) or more realistic spatial forecast 2-D (Scheme 3) in ALADIN format. Signification of exploitation of more precise Scheme 3 data is evident..

### General scheme for composition of output radiological quantities

As was mentioned above, a hypothetical radioactivity release is equivalently segmented into hourly segments  $g$ ,  $g \in \{1, 2, \dots, G\}$ . Each segment  $g$  is modelled in its subsequent

meteorological phases  $f$ ,  $f \in \{1, 2, \dots, NFAZ(g)\}$  taking into account hourly meteorological forecast.  $NFAZ(g)$  is total number of consecutive hours of the segment  $g$  tracking. Hourly plume segment  $g$  in its hourly meteorological phase  $f$  will be labelled as puf  $\{g;f\}$ . The final total values of a certain significant output  $\gamma$  at the receptor point R belonging to the effect of nuclide  $n$  is given by superposition of the results for all plume segments in their all meteorological phases according to the scheme

$${}^n\gamma_{TOTAL}(R) = \sum_{g=1}^G \left\{ \sum_{f=g}^{f=NFAZ(g)} {}^n\gamma_{\{g;f\}} \right\} \quad (7)$$

Fundamental role among simulated output categories plays four main nuclide dependent variables  $\gamma$  related to the **early phase** of an accident. Specifically, the values of  $\gamma$  can represent respectively:

- Near-ground activity concentration in air - spatial distribution around the source in polar nodes [Bq.m<sup>-3</sup>]
- Time integral of near-ground activity concentration in air – spatial distribution [Bq.s.m<sup>-3</sup>]
- Activity deposited on terrain - spatial distribution [Bq.m<sup>-2</sup>]
- Time integral of activity deposited on terrain - spatial distribution [Bq.s.m<sup>-2</sup>]

All other possible outputs  $\gamma$  like 2-D distributions of irradiation doses both in early and late stage of accident, countermeasure estimation, long-term evolution of specific activities in agricultural products and food bans effectiveness examination, long-term doses from resuspension etc. can be calculated directly from these four driving quantities applying just additional time integration. For example, estimated doses  $\Psi$  (related to the age category  $a$ ) can be schematically described as:

$$\Psi_{TOTAL}(R; a; T) \approx \sum_{n=1}^{NU} \left[ {}^n\gamma_{TOTAL}(R) \cdot I(T) \cdot {}^n\Omega^{conv}(a) \right] \quad (8)$$

$\Omega$  covers up eventual conversion factors. Time integration of long-lasting effects (e.g. radioactive decay, activity migration in soil) up to time T is formally marked as I(T). It can be usually expressed analytically. Somewhat complicated is computation of the time-integrated activity intakes according to the dynamical model of ingestion developed specially for the HARP system.

### **Fleeting glance on the probabilistic approach**

So far, we have examined simulation SGPM model under implicit assumption of the best estimated (expected) values of the model parameters. It represents simplified conceptual view of reality where the inherent uncertain features of nature are incorrectly neglected. Uncertainties of model parameters relate to imperfections of both conceptual model (algorithm limitation, simplifications during parametrization, stochastic nature of some submodel parameters, measurement errors of input data) and computational scheme (step of computation grid, averaging land-use characteristics, averaging times for dispersion parameters etc).

Before anything else we should mention different understanding between **variability** and **uncertainty** of a certain variable. Variability reflects changes of a certain quantity over time, over space or across individuals in population. Variability represents diversity or heterogeneity in a well characterized population. The term “uncertainty” covers stochastic

uncertainties, structural uncertainties representing partial ignorance or incomplete knowledge associated with lack of perfect information about poorly-characterized phenomena or models and input model uncertainties. The HARP system respects the variability concept wherever possible. The quantity with variability character is not treated as a single variable, but is split into a set of particular variables entering the calculations solo. Such an example we can mention calculation of doses, when instead of one single quantity related to all age categories of population (comprising a certain effect of inter-categorical variability) we are generating a set of values, each specific for separate age category. The distinction between perception of variability and uncertainty of meteorological inputs is crucial, as well. Seasonal and diurnal changes result in variability in meteorological data. Unlike this, we are treating as uncertainties the possible fluctuations from a certain nominal (forecasted) values of the concrete meteorological situation related to the specific time of release.

We shall return to the uncertainty treatment. In the following text the capital symbols are related to the random variable, lower case symbols stand for concrete values selected from the corresponding random distribution. Let  $\Theta \equiv [\Theta_1, \Theta_2, \dots, \Theta_M]^{-1}$  denotes a vector of  $M$  random model parameters  $\Theta_m$  with corresponding sequence of random distributions  $D_1, D_2, \dots, D_M$  which are usually selected on the basis of commonly accepted agreement of experts (range, type of distribution, potential mutual dependencies). The model parameters has usually physical meaning like initial amount of discharged radioactivity, parameters of atmospheric dispersion, uncertainties related to dry and wet fallout of radioactivity, components of wind field and many others. The expression (7) should be valid for all nodes  $R_i | i \in \{1, \dots, N\}$  of the polar computational grid. For example for 2-D spatial distribution of activity deposited on terrain the value  $N=2800$  for 35 radial distances and 80 angular sectors. Therefore, we can consider (7) in a vector form, where  $\gamma$  is a vector of dimension  $N$  with components  $\gamma_i = {}^n\gamma_{TOTAL}(R_i)$ . Having on mind the random character of the model parameters, the expression (7) can be rewritten into:

$$\Gamma = \mathfrak{R}^{SGPM}(\Theta) \quad (9)$$

where operator  $\mathfrak{R}^{SGPM}$  represents numerical algorithm SGPM outlined in (7).  $\Gamma \equiv [\Gamma_1, \Gamma_2, \dots, \Gamma_N]^{-1}$  is a vector of examined output variable  $\gamma$  with random components  $\Gamma_i$ . The unobservable random vector  $\Gamma$  is introduced into the assimilation notation as a state vector. The bold symbol  $\gamma$  stands for a vector of particular realizations of  $\Gamma$ . From a physical perspective, we can look at the (9) as a random “trajectory” of the resulting variable of interest ( $\gamma$  can stand e.g. for 2-D trajectory for trace of activity deposited on the terrain, 3-D for activity concentration in the air etc.). Analogously, the vector  $\gamma$  can be perceived as a certain concrete trajectory (given in discrete points). The sampling-based method consists in calculations of the  $k^{th}$  concrete realization  $\gamma^k$  of the state vector  $\Gamma$ , repeatedly in two steps:

- 1) Generation of a particular  $k^{th}$  sample of the parameter vector:

$$\theta^k \equiv [\theta_1^k, \dots, \theta_m^k, \dots, \theta_M^k]^{-1} \quad (10)$$

where  $\theta_m^k$  is  $k^{th}$  realisation of the  $m^{th}$  random parameter  $\Theta_m$ .

- 2) Propagation of the sample  $k$  through the model, it means the calculation of the corresponding resulting  $k^{th}$  realisation of the trajectory according to:

$$\gamma^k = \mathfrak{R}^{SGPM}(\theta_1^k, \dots, \theta_m^k, \dots, \theta_M^k) \quad (11)$$

$\gamma^k$  is the  $k^{th}$  trajectory realization, which is a vector with components  $\gamma^k_i | i \in \{1, \dots, N\}$

Adopted scheme of Monte Carlo modelling uses stratified sampling procedure LHS (Latin Hypercube Sampling). The code HARP comprise interactive subsystem for generation of  $K$  LHS samples for various types of random distributions  $D_m$  of the parameter vector  $\Theta \equiv$

$[\Theta_1, \dots, \Theta_m, \dots, \Theta_M]^{-1}$ . A certain technique for correlation control between components  $\Theta_m$  is included. Resultant mapping of pairs of vectors is given by:

$$[\boldsymbol{\gamma}^k; \boldsymbol{\theta}^k]_{k=1, \dots, K} \quad (12)$$

As described above, the trajectory  $\boldsymbol{\gamma}^k$  represents N-dimension vector of the values of quantity of interest  $\gamma$  in  $N$  spatial nodes. Provided that the value of  $K$  is sufficiently high (several thousands), the expression (12) represents the key scheme for uncertainty analysis and sensitivity studies. Statistical processing of the pairs (12) can determine the extent of uncertainty on predicted consequences and yields various statistics such sample mean and variance, percentiles of the uncertainty distribution on the quantity given, uncertainty factors, reference uncertainty coefficients etc. Simulation of uncertainty propagation through the model has a cardinal importance for introduction of advanced methods in modelling, since:

- offers essential data for transition from deterministic procedure of consequence assessment to probabilistic approach which enables to generate more informative probabilistic answers on assessment questions,
- provides detailed analysis of the model error covariance structure thus making possible to improve the reliability of model predictions on basis of application of advanced statistical techniques of assimilation of mathematical prognoses with real measurements incoming from terrain.

An example of one of the many possible modes of the probabilistic estimation is illustrated in Fig. 5 for case of hypothetical release of  $^{137}\text{Cs}$ . The release scenario with the local atmospheric precipitation, which occurred between hours 5 to 6 after the release start (random rain intensity has uniform distribution  $U[0; 6\text{mm/h}^{-1}]$ ), is described in [6].

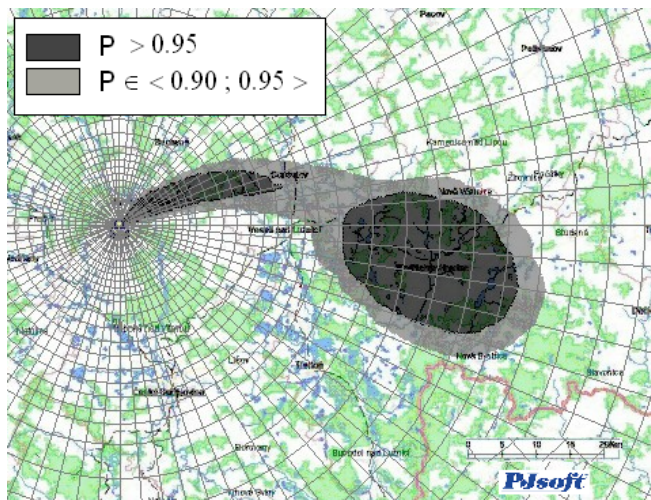


Figure 5: Isolines of probability  $P(\text{depo} > D^{\text{lim}})$  that chosen limit  $D^{\text{lim}} = 1000 \text{ Bq/m}^2$  of deposited  $^{137}\text{Cs}$  will be exceeded. Probabilistic SGPM analysis includes 5000 random samples. Retrospective meteorological forecast sequence from June 28, 2002 with release start at 00 UTM was used. Highly contaminated area in far distance is caused by the local atmospheric precipitation, which occurred between hours 5 to 6 after the release start (random rain intensity has uniform distribution  $U[0; 6\text{mm h}^{-1}]$ ).

### Data assimilation – true way from model to reality

Due to complexity of the problem and uncertainties involved we can never succeed only with standalone computer codes, even being as sophisticated as possible. Any model of pollution transport is always a simplified picture of reality. In can not comprise all features of the real world both from theoretical and practical reasons. In its full formulation, the system of equations for atmospheric state has stochastic character and describes the dynamic chaos. As

a consequence, the predictability of evolution of the weather conditions is limited. The solution is provided by the data assimilation procedures that accomplish an optimal blending of all information resources including prior physical knowledge given by model, observations incoming from terrain, past experience, expert judgment and intuition.

Bayesian approach to estimation of unknown quantities  $\Gamma_t$  is based on recursive evaluation (in discrete time steps  $t$ ) of posterior probability density  $p(\Gamma_t | Y_t)$  using the Bayes rule:

$$\text{Prediction step:} \quad p(\Gamma_t | Y_{t-1}) = \int p(\Gamma_t | \Gamma_{t-1}) p(\Gamma_{t-1} | Y_{t-1}) d\gamma_t \quad (13a)$$

$$\text{Data update step:} \quad p(\Gamma_t | Y_t) \propto p(y_t | \Gamma_t) p(\Gamma_t | Y_{t-1}) \quad (13b)$$

In the prediction step the prior probability density function  $p(\Gamma_t | Y_{t-1})$  is estimated. It stands for probability of the state  $\Gamma_t$  given  $Y_{t-1}$ . The probability  $p(y_t | \Gamma_t)$  represents the *pdf* of measurement set incoming at  $t$  given state  $\Gamma_t$ . Symbol  $\propto$  denotes equality up to multiplicative constant. The sets of observations incoming from the same beginning in each time step of recursion up to the time interval  $t$  is arranged into the array  $Y_t = [y_1, y_2, \dots, y_t]$ .

Our contribution in the field insists in development and application of an advanced statistical method of the particle filtering (PF) based on Bayesian filtration [4]. The 3-dimensional state trajectories (particles), standing for realisations  $k, k \in \{1, \dots, K\}$  of random system state, remains unchanged during the data (observations) update step and only their weights  $w_t^k$  are updated. Thus, the history of each path is not lost and the next time update is straightforward even using the trajectory algorithm SGPM. The PF originating from the family of sequential Monte Carlo methods is applied here for simulation of the **posterior distribution** of the system state. During the resampling recursive procedure, those particles having small weights with regard to the measurements are eliminated. An arbitrary moment  $m(\Gamma_t)$  of the multidimensional *pdf* is then easily evaluated by a summation:

$$m(\Gamma_t) = \sum_{k=1}^K w_t^k \cdot m(\gamma^k) \quad (14)$$

For demonstration of the PF application we have adjusted the following accidental scenario. Real meteorological situation from March 31, 2009 is taken into consideration and the moment of hypothetical radioactivity release is set to 10.00 UTC. Available real meteorological observations measured near the point of NPP Temelin and corresponding short term meteorological forecast are somewhat inconsistent (see Table 1).

*Table 1: A hypothetical accidental release scenario of  $^{131}\text{I}$ . Short-term meteorological forecast and real meteorological measurements (in brackets) for "point" of NPP Temelin ( $49^\circ 10' 48.53''\text{N} \times 14^\circ 22' 30.93''\text{E}$ ), time stamp 20090331-1000 UTC.*

UTC hour	10.00	11.00	12.00	13.00	....
activity release of $^{131}\text{I}$ Bq/h	$5.68 \times e+14$	$7.92 \times e+14$	0	0	....
wind direction <sup>1),2)</sup>	95.0 ( 69.0 )	101.0 ( 65.0 )	84.0 ( 80.0 )	80.0 ( 64.0 )	....
wind speed <sup>1)</sup> m.s <sup>-1</sup>	2.0 ( 3.0 )	2.1 ( 3.3 )	1.9 ( 3.8 )	2.2 ( 4.0 )	....
Pasquill class of atm. stabil.	A	A	B	B	....

<sup>1)</sup> at 10 m heigh; <sup>2)</sup> degrees measured clockwise from North

The following ex post analysis can give a retrospective view on such atypical situations (their occurrence rate is surprisingly not negligible). The evolution of emergency situation from the same beginning of an accident is usually so far varied and complicated that specific ad hoc solutions have to be introduced. The numerical experiment described in [4] is conducted as a twin experiment, where the measurements are simulated via a twin model and perturbed. Following the eq.(11), the deterministic ("best estimated") trajectory  $\gamma^{\text{best}}$  can be expressed as:

$$\gamma^{\text{best}} = \mathfrak{R}^{\text{SGPM}}(\theta_1^{\text{best}}, \theta_2^{\text{for}}, \theta_3^{\text{for}}, \dots) \quad (15)$$

Let  $\theta_1^{\text{best}}$  stands for initially estimated value of the release source strength in the first hour,  $\theta_2^{\text{for}}, \theta_3^{\text{for}}$  represent values of wind direction and wind velocity forecasted by ALADIN model for the first hour. Following the table 1,  $\theta_1^{\text{best}} = 5.68\text{E}+14$  Bq,  $\theta_2^{\text{for}} = 95.0$  deg,  $\theta_3^{\text{for}} = 2.0$  m.s<sup>-1</sup>. For the probabilistic calculations their random character is expressed in standardized form  $\Theta_1 = \theta_1^{\text{best}} \cdot C_1$ ,  $\Theta_2 = \theta_2^{\text{for}} + C_2 \cdot \Delta\varphi^{\text{fix}}$ ,  $\Theta_3 = \theta_3^{\text{for}} \cdot C_3$  etc. (see [4]).  $C_1$ ,  $C_2$  and  $C_3$  are standardized random parameters having distribution determined on basis of expert judgement:

$$\begin{aligned} C_1 &\in \langle 0.31; 3.1 \rangle, & \text{LogUniform pdf}(c_1), & \text{median} = 1.0 \\ C_2 &\in \langle -12.0; +12.0 \rangle & \text{Uniform pdf}(c_2), & \text{median} = 0.0, \Delta\varphi^{\text{fix}} = 4.5 \text{ deg} \\ C_3 &\in \langle 0.5; 3.0 \rangle & \text{Uniform pdf}(c_3) & \end{aligned} \quad (16)$$

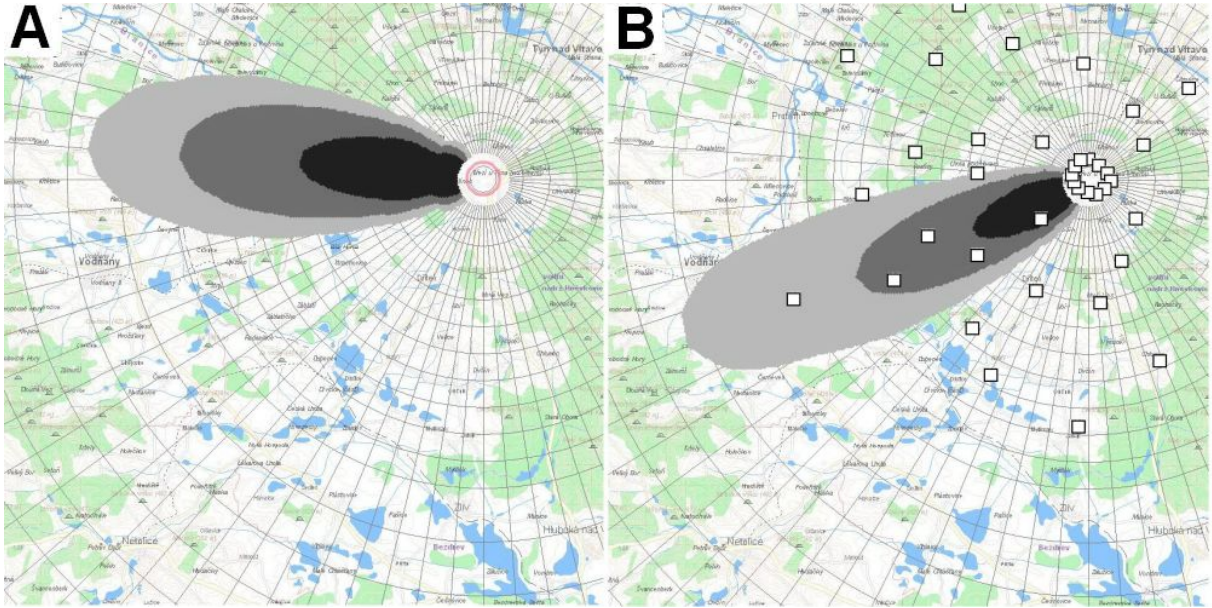


Figure 6: <sup>131</sup>I deposition according to the SGPM model performed with “best estimate” (nominal) values of model parameters. The situation just after 2 hours from the beginning of the release.

**A** – Meteorology according to the short term meteorological forecast (ALADIN) from Table 1;

**B** – Meteorology according to the real measurements (in brackets in Table 1); White squares behind NPP areal boundary represent selected dummy measurement stations.

Specifically, the “artificial” measurements in nearest vicinity are intended for TDS on the NPP areal boundary (24 positions). The rest of 54 measurement points (white squares in Figure 6-B) are generated in the positions selected deliberately with regard on the experiment purpose. This “measurements” are taken from the “observation” trajectory  $\gamma^{\text{obsv}}$  calculated by the same environmental model (deterministic version of the HARP code) using the real meteorological measurements near the point of NPP (see Table 1 – values in brackets) :

$$\gamma^{\text{obsv}} = \mathfrak{R}^{\text{SGPM}}(\theta_1^{\text{obsv}}, \theta_2^{\text{obsv}}, \theta_3^{\text{obsv}}, \dots) \quad (17)$$

For the further demonstration of the DA capabilities (see below) was chosen  $\theta_1^{\text{obsv}} = 0.5 \cdot \theta_1^{\text{best}}$ . The last two parameters represent the real meteorological measurements according to Table 1, the values in brackets,  $\theta_2^{\text{obsv}} = 69.0$  deg,  $\theta_3^{\text{obsv}} = 3.0$  m.s<sup>-1</sup>. The projection of the  $\gamma^{\text{best}}$  resp  $\gamma^{\text{obsv}}$  trajectories into 2-D representation of <sup>131</sup>I deposition are illustrated in Fig. 6 A resp 6 B.

The essential results of PF application are shown in Figure 7. Bayesian update step assimilates the first batch of  $^{131}\text{I}$  deposition measurements (let incoming just after 2 hours from the release start) and enables estimation of the posterior probability density function *pdf*. Its expectations given in Figure 7 A illustrate the way how to easily estimate the moments of the extremely complicated multidimensional state *pdf*, which is not tractable analytically. The expectation values from Fig. 7 A are determined according to summation (14) and, in fact, stand for mean values weighted by weights resulting from the PF assimilation technique. The PF weights result from advanced statistical treatment based on SMC modelling. A tendency to lean to either model predictions (e.g. Fig. 6 A) or measurements (Fig. 7 B) are mapping by proper treatment of covariance matrices of model and measurements errors. From this point of view, the results in Figure 7 A reflect our strong confidence to precision of the observed values incoming from terrain.

The evidence of SGPM capability to execute the time update step (13a) of the Bayesian recursion is given in Figure 7 B. The most suitable “trajectories”, which have formed the results in Figure 7A, are properly proliferated and each of them is extended from the state valid for the second hour (Fig. 7 A) to the next hour 3. The results expressed in the form of prior *pdf* expectation related to the hour 3 are illustrated in figure 7 B. Then, the Bayesian recursion can run on the next assimilation cycle. The segmented Gaussian model SGPM gives promising results for online plume tracking and seems to be fast enough to offer the improved predictions of impacted areas to decision-making timely.

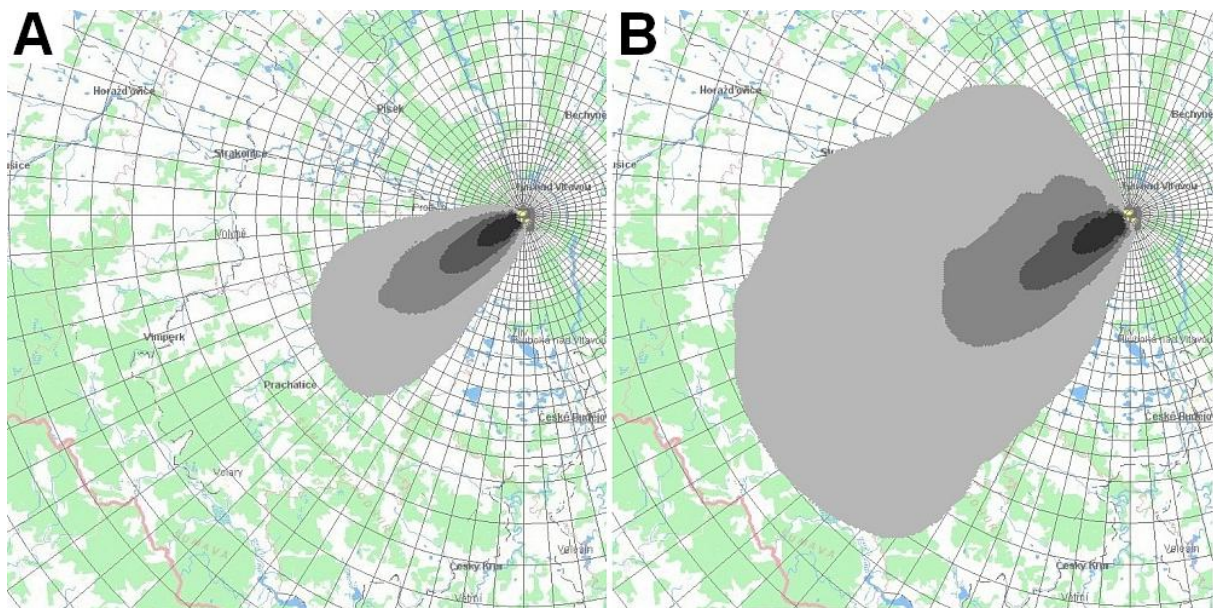


Figure 7: **A** - Expectations of posterior *pdf* of the radioactivity deposition (just after two hours after the start when incoming measurements were assimilated). **B** – Prediction of the state one hour forward: prior *pdf* expectations for transition from hour 2 to hour 3.

Inherent feature of the PF methodology is collateral re-estimation of actual values of the important model parameters, as are the release source strength, dispersion parameters, dry deposition velocity and washing of activity from the cloud caused by atmospheric precipitation or components of wind field. An example for the first three random parameters  $C_1$ ,  $C_2$  and  $C_3$  (the priors are defined according to eq. (16) ) is given in Figure 8. Knowledge comprised in the observations from terrain leads to the significant sharpening of the posterior histograms distributed near the selected observation values  $c_1^{\text{obsv}}=0.5$ ,  $c_2^{\text{obsv}} = (69.0 - 95.0)$

$\Delta\varphi^{\text{fix}} = -7.6$ . It follows from expressions  $\theta_1^{\text{obsv}} = c_1^{\text{obsv}} \cdot \theta_1^{\text{best}}$ ,  $\theta_2^{\text{obsv}} = \theta_2^{\text{for}} + c_2^{\text{obsv}} \cdot \Delta\varphi^{\text{fix}}$  and from values in Table 1. The fuzzy results for posterior histogram of  $C_3$  (wind velocity during the first hour of release) is connected with deficiency of observations at longer distances from the source (see experimental distribution of measurement stations in Figure 6 B). Thus, the originally theoretical assimilation research can impose well-founded recommendations on spatial resolution of measurement stations.

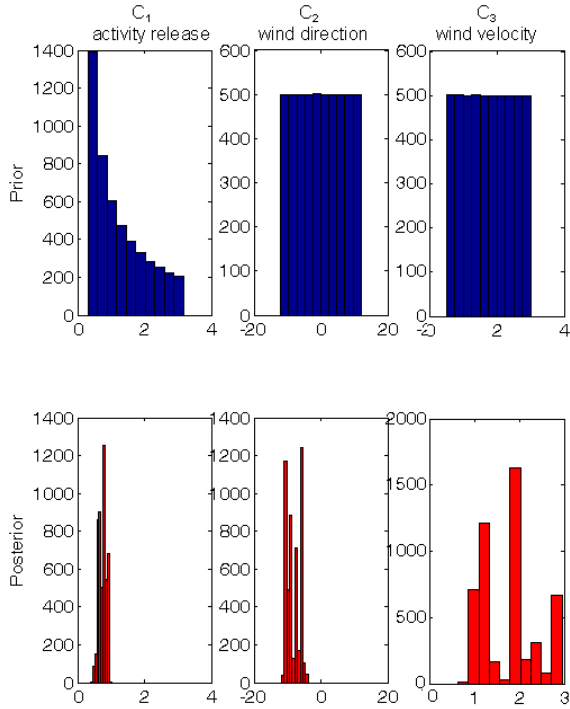


Figure 8: Comparison of prior (top row) and posterior (bottom row) histograms of distribution of selected random parameters  $C_1, C_2, C_3$  - see definition in equation (16).

## Conclusion

- The main features of the environmental system HARP were introduced. The system is capable to adopt the latest format of meteorological data and simulate dynamics of the releasing activity. It offers an advanced interactive tool for estimation of consequences of an accident from the initial phase of radioactivity release into atmosphere and its further transport through the living environment up to human body. Important unresolved issues of advection- dispersion transport are connected with fast changes of atmospheric stability, treatment of inversion situations, transport over the complex terrain and urban areas and analysis of calm situations.
- Fast and sufficiently accurate SGPM algorithm together with online connection to meteorological forecast and archive of the meteorological data make now feasible also computationally intensive calculations. For instance, the PSA-Level3 analysis using retrospective true meteorological data actually valid for each hour in a year can be accessed and executed. The final statistical preprocessing can quantify the variability due to meteorological changes (diurnal, seasonal etc.). Another promising result has been achieved in the assessment of long-term radiological consequences due to the normal

operation of NPP. Practicability of the HARP code for the future EIA studies has been confirmed.

- The probabilistic modelling of uncertainty propagation through the model provides right basis for the uncertainty and sensitivity analysis and introduction of advanced procedures of consequence assessment. It ensures to follow the recent trends in risk assessment methodology insisting in transition from deterministic procedures to probabilistic approach which enables to generate more informative probabilistic answers on assessment questions.
- The most important achievement insists in development of a special data assimilation techniques and their application in the early and late stages of radiation accident. The adopted procedure of the Particle Filter seems to be robust enough and suitable to manage a certain discrepancies and scenario incompleteness occurring from the same beginning of an accident. Nesting of the data assimilation cycles within the predictions in the particular time steps seems to be crucial for an improvement of emergency preparedness.
- In the field of data assimilation progressions, many questions remain opened. Important problems relate to availability and accessibility of measurements, namely establishing a dialogue and cooperation with proper providers of data from radiation monitoring networks, solving interrelationship of measured data correspondence and conformance with generated model outputs (direct or indirect measurements), discriminating between modes of incoming observations (intermittent or continuous), accounting for measurement errors and density of measurement stations coverage on terrain etc.

## Acknowledgement

This work was supported by grant project GAČR No. 02/07/1596. The authors thank to colleagues from working group MEDARD from the Institute of Computer Science, AV ČR, for their help with MM5 gridded meteorological data format during the tests of potential utilisation of knowledge from the Lagrangian model HYSPLIT.

## Acronyms and symbols

ADM	Atmospheric Dispersion Model
ALADIN	model of numerical weather forecast on limited 3-D area
CET	Central European Time
DA	Data Assimilation
DEP	DEPosited radioactivity on terrain
EIA	Environmental Impact Assessment
FCM	Food Chain Model
$\Gamma_t$	random state vector
HARP	Hazardous Radioactivity Propagation program system
K	number of stratified samples of vector of input parameters
LHS	Latin Hypercube Sampling scheme
M	number of input model parameters considered in the HARP code as random
MM5	Numerical weather Mesoscale Model of 5 <sup>th</sup> generation
N	dimension of background vector (number of polar nodes of computational grid)
NPP	Nuclear Power Plant
<i>pdf</i>	probability density function
$p(y_t / \Gamma_t)$	conditional <i>pdf</i> of measurement set $y_t$ at $t$ given state $\Gamma_t$
PF	assimilation technique of Bayesian Particle Filtering
PSA	Probabilistic Safety Assessment
RDD	Radiological Dispersion Device
SGPM	Segmented Gaussian Plume Model

SMC	Sequential Monte Carlo methods
TDS	TeleDosimetric System
TIC	Time Integral of near-ground specific activity Concentration in air
UA, SA	Uncertainty Analysis, Sensitivity Analysis
UTC	Universal Time Coordinated

## References

- [1] A. Doucet, N. De Freitas and N.J. Gordon (eds.): *Sequential Monte Carlo method in practice*. Springer-Verlag, New York, 2001.
- [2] R. R. Draxler, G. D. Hess: Description of the HYSPLIT\_4 Modelling System. NOAA Tech. Memorandum, ERL ARL-224, rev. 2004.
- [3] P. Kuča, R. Hofman and P. Pecha: Assimilation techniques in consequence assessment of accidental radioactivity releases – the way for increase of reliability of predictions. In Proc. of ECORAD 2008, Bergen, Norway, June 15-20, 2008, 138-141.
- [4] P. Pecha, R. Hofman, V. Šmídl: Bayesian tracking of the toxic plume spreading in the early stage of radiation accident. In Proc. of European Simul. and Modelling Conference ESM'2009, Leicester, UK, Oct. 26-28, 2009, pp. 381-387.
- [5] P. Pecha, E. Pechová and R. Kelemen: Application of system HAVAR-RP in the field of radiation protection. HAVAR-RP archive, 2006, rev. 2009. In the Czech.
- [6] P. Pecha, R. Hofman. HARP - A Software Tool for Decision Support during Nuclear Emergencies. TIES 2009 - The 20th Annual Conference of International Environmetrics Society, Handling Complexity and Uncertainty in Environmental Studies, (Bologna, IT, July 5-7, 2009).
- [7] P. Pecha, R. Hofman, E. Pechová : Training simulator for analysis of environmental consequences of accidental radioactivity releases. In Proc. of the 6th EUROSIM Congress on Modelling and Simulation , Eds: Zupančič Borut, Ljubljana, SI, Sept. 9 – 13, 2007.
- [8] R. Hofman, P. Pecha, E. Pechová : A Simplified Approach for Solution of Time Update Problem during Toxic Waste Plume Spreading in the Atmosphere. In Proc. of HARMO12-12<sup>th</sup> Inter. Conf. on Harmonization within Atmospheric Dispersion Modelling for Regulatory Purposes, Hrvatski Meterološki Časopis, Paper No. H12-57, pp. 510-515, Cavtat, HR, Oct. 6 -10, 2008.
- [9] P. Kuča, P. Pecha and R. Hofman : Lessons learned from former radiation accidents on development of software tools for effective decision making support. In Proc. of 11<sup>th</sup> In. Conf. on Present and Future of Crisis Management. Praha, CZ, Nov. 23 – 24, 2009, ISBN 978-80-254-5913-3.